ENVIRONMENTAL RESEARCH
LETTERS

LETTER • OPEN ACCESS

Crop-specific exposure to extreme temperature and moisture for the globe for the last half century

To cite this article: Nicole D Jackson *et al* 2021 *Environ. Res. Lett.* **16** 064006

ENVIRONMENTAL RESEARCH
LETTERS

LETTER

Crop-specific exposure to extreme temperature and moisture for the globe for the last half century

Nicole D Jackson[1], Megan Konar[1], Peter Debaere[2] and Justin Sheffield[3]

[1] Department of Civil and Environmental Engineering, University of Illinois at Urbana-Champaign, Urbana, IL 61821, United States of America
[2] Darden School of Business, University of Virginia, Charlottesville, VA 22903, United States of America
[3] Geography and Environmental Science, University of Southampton, Southampton, United Kingdom

E-mail: mkonar@illinois.edu

OPEN ACCESS

RECEIVED
14 December 2020

REVISED
17 March 2021

ACCEPTED FOR PUBLICATION
16 April 2021

PUBLISHED
17 May 2021

Keywords: crop-specific, weather extremes, temperature, moisture, global, gridded, time series

Supplementary material for this article is available online

Abstract

Global assessments of climate extremes typically do not account for the unique characteristics of individual crops. A consistent definition of the exposure of specific crops to extreme weather would enable agriculturally-relevant hazard quantification. To this end, we develop a database of both the temperature and moisture extremes facing individual crops by explicitly accounting for crop characteristics. To do this, we collate crop-specific temperature and moisture parameters from the agronomy literature, which are then combined with time-varying crop locations and high-resolution climate information to quantify crop-specific exposure to extreme weather. Specifically, we estimate crop-specific temperature and moisture shocks during the growing season for a 0.25° spatial grid and daily time scale from 1961 to 2014 globally. We call this the Agriculturally-Relevant Exposure to Shocks (ARES) model and make all ARES output available with this paper. Our crop-specific approach leads to a smaller average value of the exposure rate and spatial extent than does a crop-agnostic approach. Of the 17 crops included in this study, 13 had an increase in exposure to extreme heat, while 9 were more exposed to extreme cold over the past half century. All crops in this study show a statistically significant increase in exposure to both extreme wetness and dryness. Cassava, sunflowers, soybeans, and oats had the greatest increase in hot, cold, dry, and wet exposure, respectively. We compare ARES model results with the EM-DAT disaster database. Our results highlight the importance of crop-specific characteristics in defining weather shocks in agriculture.

1. Introduction

Extreme weather (also called 'shocks' and 'hazards') negatively impacts agricultural yield and total factor productivity [1–7]. Weather shocks are projected to increase in both frequency and severity in the future [8, 9], making it important to better understand the relationship between extreme weather and agriculture. In recent years, there has been a dramatic increase in research to evaluate extreme weather in agriculture [10–13]. However, there is still a need for a historical assessment of extreme weather that accounts for the characteristics of specific crops and includes both temperature and moisture extremes. The goal of this paper is to develop a consistent definition of crop-specific exposure to extreme temperature (e.g. too hot and too cold) and moisture (e.g. too wet and too dry) and consistently evaluate its spatial and temporal trends at the global scale for the past half century.

Prior work has evaluated extreme weather in agriculture [14, 15]. It is increasingly being recognized that crops have distinct physiological thresholds that lead them to be impacted differently by the same weather. This means that some crops are more sensitive than others [16, 17]. For example, corn yields were shown to increase with temperature up to 29°C in the United States, while soy has a higher threshold of 30°C and cotton has an even higher threshold of 32°C [18]. Yet, most work to

quantify weather extremes in agriculture has been agnostic to crop type, particularly in terms of moisture demands [12, 19]. Studies that do distinguish by crop type typically focus on specific regions of the world, rather than considering the entire globe [18], or a small number of crops [10, 17, 20]. Likewise, extremes occur at both tails of the distribution [20–23], making it important to evaluate exposure to temperatures that are both too hot and too cold, as well as moisture stress from soil that is too wet and too dry [11, 24]. However, many studies focus on a single tail of the distribution, such as drought [15, 25, 26] or extreme heat [16, 27]. There is thus a need to develop a crop-specific definition of climate extremes and evaluate it for a comprehensive range of locations, times, extremes, and crops.

A consistent definition of crop-specific climate extremes would enable a retrospective analysis of how these events have changed over time. This approach would improve upon the Emergency Events Database (EM-DAT), which many studies that seek to examine the relationship between extreme weather and agriculture rely upon [11]. EM-DAT is a country-level self-reported database of extreme events. However, the fact that EM-DAT is self-reported is problematic, because some countries may be more likely to report extreme events in agriculture than others, leading to bias in the dataset. Additionally, EM-DAT has broad representation of disasters, but was not specifically designed to represent the unique features of agricultural extremes. EM-DAT also reports events with significant economic impact rather than consistently defined occurrence of hazards. This makes it difficult to compare climate hazards in agriculture across countries and through time using the EM-DAT database. For this reason, the goal of this paper is to consistently define agricultural extremes by crop across space and time.

Prior work to determine the interaction between weather and agriculture has been hampered by a coarse understanding of where crops are grown. At the country spatial scale, time series information on the locations of specific crops is available from the Food and Agriculture Organization. However, for gridded land cover, many studies rely on estimates of crop locations circa 2000 (e.g. as provided by [28]) with time-varying climate information [25]. These approaches would likely be improved by including time-varying estimates of gridded crop locations. To this end, we incorporate annual crop location maps from the Probabilistic Cropland Allocation Model (PCAM) [29]. PCAM gridded crop maps are available at the annual time step from 1960 to 2014.

In this study, we define crop-specific exposure to climate shocks. To do this, we draw upon the agronomy literature and collate crop parameters for critical temperatures and moisture demands. We fuse these agronomic parameters with detailed climate information to define crop-specific exposure to climate extremes. To determine where specific crops are located in each year of the study, we use PCAM [29]. We develop the Agriculturally-Relevant Exposure to Shocks (ARES) model to estimate crop-specific exposure to extreme weather. We use ARES to quantify historical exposure to extreme temperature (too hot and too cold) and moisture (too wet and too dry) by crop for 17 crops for the globe from 1961 to 2014. This enables us to ask the following scientific questions: (a) How does our understanding of extreme weather in agriculture change with a crop-specific approach? (b) How has the exposure of certain crops to extreme weather changed over time? (c) What is the spatial distribution of weather shocks around the world?

Table 1. Summary of gridded datasets used in this study.

Source	Spatial scale	Time period	Variable collected
Sheffield *et al* [32]	0.25°	1961–2014	Daily maximum temperature, minimum temperature, precipitation and reference evapotranspiration
Jackson *et al* [29]	0.5°	1961–2014	Probabilistic estimates of crop-specific areas
Sacks *et al* [34]	5 arc min	2000	Primary and secondary crop calendars

2. Methods

We develop the ARES model to consistently evaluate the evolution of extreme events to specific crops. ARES is built by integrating multiple data sources (see table 1). In general, our approach begins with global gridded climate data that is winnowed by crop-specific agronomic thresholds to identify crop-specific thermal and hydrologic extreme events in time and space. Figure 1 provides an overview of our model framework. The ARES approach presents a consistent shock definition that is used to quantify crop-specific exposure to extreme events as a time-varying, gridded product. The following subsections provide details on the data sources, event construction, model assessment, and critical assumptions.

2.1. Data sources and integration

ARES is based upon multiple global gridded datasets as well as crop-specific agronomic information. Table 1 summarizes the global gridded data products used in this study. We collate information on crop-specific temperature thresholds in table 2. T_{min} represents the minimum temperature beyond which the yield of that crop will decline; T_{max} indicates the maximum temperature beyond which yield declines will occur. T_{opt} shows the optimum temperature for crop growth. Three critical temperatures are

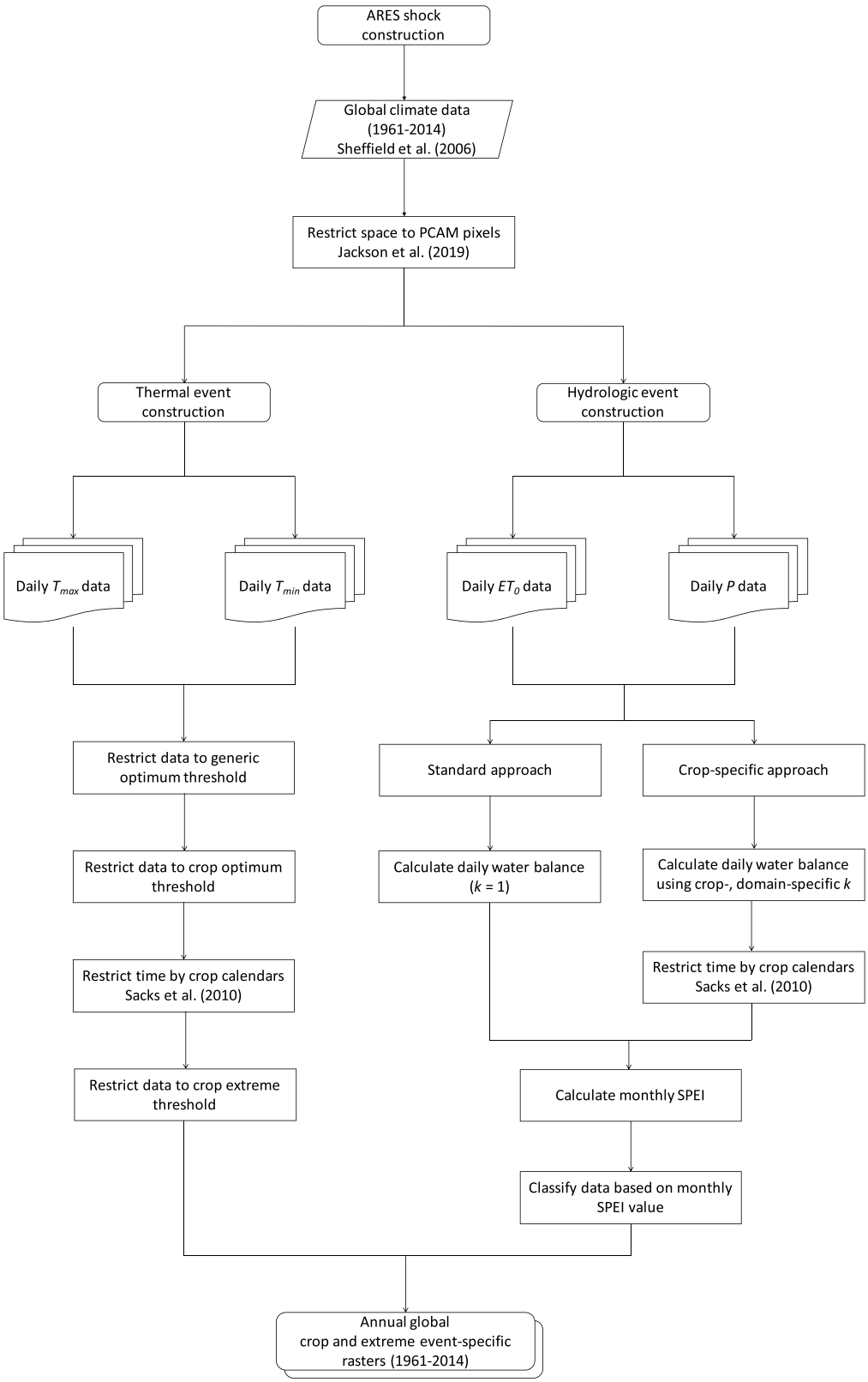

Figure 1. Schematic of the ARES methodology. T_{max} refers to maximum temperature, T_{min} is minimum temperature, ET_0 is reference evapotranspiration, and P is precipitation.

determined for each crop in this study: minimum, optimum, and maximum. These thresholds were collected from dozens of research articles through a literature review that builds on previous efforts by Porter and Gawith [30], as well as Hatfield and Prueger [31]. When multiple values were found for the same threshold we averaged the values to obtain the threshold presented in table 2. We provide the full citation list for the agronomic research that we drew from in the supporting information (SI) (available online at stacks.iop.org/ERL/16/064006/mmedia).

Table 2. Physiological crop thresholds and coefficients applied in this study. The crop coefficients are adapted from Doorenboos and Pruitt [36] for the initial (ini), middle (mid), and endpoints (end) of the growing season. Seasons are identified as 'M' for main, 'S' for secondary, and 'W' for winter.

			Thermal threshold (°C)			Crop coefficient		
Crop	Species	Season	T_{min}	T_{opt}	T_{max}	k_{ini}	k_{mid}	k_{end}
Barley	Hordeum vulgare	M	0.7	18.3	33.1	0.3	1.15	0.25
Barley		W	−12.0	11.5	33.0	0.3	1.15	0.25
Cassava	Manihot esculenta	M	15.0	27.0	45.0	0.3	0.95	0.725
Groundnuts	Arachis hypogaea	M	13.1	27.0	40.5	0.4	1.15	0.6
Maize	Zea mays	M	6.2	30.8	42.0	0.3	1.2	0.475
Maize		S	6.2	30.8	42.0	0.3	1.2	0.475
Millet	Panicum miliaceum	M	10.7	32.5	43.8	0.3	1	0.3
Oats	Avena sativa	M	−3.9	17.8	23.0	0.3	1.15	0.25
Oats		W	−4.8	11.3	23.0	0.3	1.15	0.25
Potato	Solanum tuberosum	M	−3.7	15.1	27.0	0.5	1.15	0.75
Rapeseed	Brassica napus	W	3.8	20.9	28.3	0.35	1.075	0.35
Rice	Oryza sativa	M	13.5	27.6	35.4	1.05	1.2	0.75
Rice		S	13.5	27.6	35.4	1.05	1.2	0.75
Rye	Secale cereale	W	−5.4	12.5	30.0	0.3	1.15	0.4
Sorghum	Sorghum bicolor	M	9.5	31.0	36.9	0.3	1.05	0.55
Sorghum		S	9.5	31.0	36.9	0.3	1.05	0.55
Soybeans	Glycine max	M	11.4	28.3	39.4	0.4	1.15	0.5
Sugarbeet	Beta vulgaris	M	−1.6	20.3	32.8	0.35	1.2	0.7
Sunflowers	Helianthus annuus	M	7.4	29.4	43.1	0.35	1.075	0.35
Sweet Potato	Ipomoea batatas	M	14.9	28.9	40.0	0.5	1.15	0.65
Wheat	Triticum aestivum	M	6.4	21.6	28.7	0.3	1.15	0.325
Wheat		W	1.0	14.3	28.5	0.55	1.15	0.325
Yams	Dioscorea alata	M	14.8	25.2	37.4	0.5	1.1	0.95

We obtain an update to the Princeton Global Meteorological Forcing dataset [32, 33] for the period 1961–2014 for the following climate variables: maximum temperature (T_{max}), minimum temperature (T_{min}), precipitation (P), and reference evapotranspiration (ET_0). These variables enable us to calculate extremes in both temperature and moisture conditions. Note that these variables are obtained at the 0.25° spatial resolution and daily time-step.

Global gridded crop calendars are obtained from Sacks *et al* [34] at the 5 arcmin spatial resolution. The data is interpolated to a 0.25° spatial resolution to match the climate data. These calendars provide us with information on which Julian day planting, growing, and harvesting periods have started and ended. We treat the period from the end of planting to the start of harvesting as the growing season. A binary indicator is used to identify whether or not a given day occurs during the agricultural calendar. Note that Sacks *et al* [34] provide information on multiple growing seasons for certain crops when applicable (see table 2), which we include in this study. Distinct growing seasons are treated independently (e.g. the extreme events that occur in each growing season are tabulated individually). Annual extreme event values for crops with multiple growing seasons are summed across all growing seasons.

It is particularly important to refine crop growth phases to assess moisture extremes in crop production. The length of each crop's growth stages is obtained from Doorenbos and Pruitt [35]. We averaged the lengths across all regions for each crop and use proportionality to assign agriculture calendar days to each growth stage. This enables us to apply crop coefficients from Doorenbos and Pruitt [36] that vary by growth stage to the correct days within the agriculture calendar of each crop. Crop coefficients for the development growth stage are estimated by averaging coefficients for the initial and middle stages. Similarly, the late growth stage coefficients are averages of the middle and endpoint coefficients.

We obtain crop-specific locations from the Probabilistic Cropland Allocation Model (PCAM) [29] for the period 1961–2014 at 0.5° spatial resolution. We downscale PCAM data to 0.25° spatial resolution to match the climate data. Each pixel's unique latitude-longitude pairing allows us to construct annual crop-specific panels that integrate climate, crop calendar, and land use data.

2.2. Thermal event exposure

We quantify both extreme cold and hot temperature events annually. We do this by tracing through a series of phases to derive crop-specific thermal event exposure rates (see figure 1). The goal is to winnow the database from generic (e.g. not crop-specific) thresholds to crop-specific extremes that occur only during the growing season. The approach is based on a modification of the process developed by Teixeira *et al* [27] and is summarized as follows:

- Phase T1: restrict climate data to a generic optimal threshold

- Phase T2: restrict climate data to the crop-specific optimum threshold
- Phase T3: restrict climate data in time by crop calendars
- Phase T4: restrict climate data with crop-specific extreme threshold
- Phase T5: repeat phases 1–4 for all crops, seasons, and years in the study domain

Throughout the phases, we use the daily maximum and minimum temperatures as it is consistent with approaches used by Zhu and Troy [12], Lobell *et al* [37], and Barlow *et al* [38]. The following are additional details on each of the thermal event phases:

Phase T1: restrict climate data to a generic optimum threshold. The threshold for phase T1 is based on a generic value across all crops per season. The generic optimum is equal to the minimum seasonal optimal value for maximum temperature events, and the maximum optimal value for minimum temperature events (see table 2 and equation (1)). Equation (1) presents the sample binary indicator to identify events at the generic thermal threshold:

$$f_{T_{1,p,d,y,\mathrm{crop}}} = \begin{cases} 1, & \text{if } T_{\max,p,d,y} > \min(T_{\mathrm{opt,crop,season}}) \\ 1, & \text{if } T_{\min,p,d,y} < \max(T_{\mathrm{opt,crop,season}}) \\ 0, & \text{otherwise} \end{cases} \tag{1}$$

where $f_{T_{1,p,d,y,\mathrm{crop}}}$ is the resulting binary indicator for phase T1 at pixel p, $T_{\max,p,d,y}$ is the pixel p's maximum temperature on day d for year y, $T_{\min,p,d,y}$ is pixel p's daily minimum temperature, and $T_{\mathrm{opt,crop,season}}$ are the crop- and season-specific optimum temperatures presented in table 2. The minimum optimal values for maximum temperature are 15.05 °C, 27.6 °C, and 11.25 °C for main, secondary, and winter seasons, respectively. The maximum optimal values for minimum temperature are 32.47 °C, 30.97 °C, and 20.88 °C for main, secondary, and winter seasons, respectively.

Phase T2: restrict climate data to the crop-specific optimum threshold. The threshold for phase T2 is the crop-specific optimum temperature ($T_{\mathrm{opt,crop,season}}$) for the given season (see table 2). Equation (2) presents the binary specification for this phase, $f_{T_{2,p,d,y,\mathrm{crop}}}$:

$$f_{T_{2,p,d,y,\mathrm{crop}}} = \begin{cases} 1, & \text{if } T_{\max,p,d,y} > T_{\mathrm{opt,crop,season}} \\ 1, & \text{if } T_{\min,p,d,y} < T_{\mathrm{opt,crop,season}} \\ 0, & \text{otherwise} \end{cases} \tag{2}$$

Phase T3: restrict climate data in time by crop calendars. The calendar dataset from Sacks *et al* [34] provides crop- and season-specific, pixel-level information on the first day of planting ($d_{p,\mathrm{crop,PS}}$) through the last day of harvest ($d_{p,\mathrm{crop,HE}}$). These date ranges are used for each year (y) of the study domain. Equation (3) presents the binary specification for this phase, $f_{T_{3,p,d,y,\mathrm{crop}}}$. Note that there is both a temperature requirement and time requirement in this specification that must be met on each day (d) in the year (y) for the given pixel (p) and crop

$$f_{T_{3,p,d,y,\mathrm{crop}}} = \begin{cases} 1, & f_{T_2} = 1 \;\&\; d_{p,\mathrm{crop,PS}} \le d \le d_{p,\mathrm{crop,HE}} \\ 0, & \text{otherwise} \end{cases} \tag{3}$$

where PS is plant start date and HE is harvest end.

Phase T4: restrict climate data to the crop-specific extreme threshold (i.e. the minimum and maximum values provided in table 2). For maximum temperature events, the thermal threshold is equivalent to the crop-specific maximum temperature. For minimum temperature events, the extreme threshold is the minimum of the frost temperature (0 °C) and the crop- and season-specific minimum temperature. Equation (4) presents the binary specification for this phase, $f_{T_{4,p,d,y,\mathrm{crop}}}$:

$$f_{T_{4,p,d,y,\mathrm{crop}}} = \begin{cases} 1, & f_{T_{3,p,d,y,\mathrm{crop}}} = 1 \;\&\; T_{\max,p,d,y} > T_{\mathrm{max,crop,season}} \\ 1, & f_{T_{3,p,d,y,\mathrm{crop}}} = 1 \;\&\; T_{\min,p,d,y} < \min\left(T_{\mathrm{min,crop,season}}, 0\,^{\circ}\mathrm{C}\right) \\ 0, & \text{otherwise.} \end{cases} \tag{4}$$

The daily events determined by equations (1)–(4) are aggregated to calculate annual, crop-specific, pixel-level exposure rates as defined by equation (5). Phases T1 and T2 are summed across the calendar year where the number of days in a year (D) is 365 or 366 days depending on whether the year (y) is a leap year or not. Phases T3 and T4 are summed across the growing season such that $G_{p,\mathrm{crop}}$ is the total number of days between planting start date ($d_{p,\mathrm{crop,PS}}$) through the harvest end date ($d_{p,\mathrm{crop,HE}}$) for a crop likely grown in pixel p. For crops with multiple growing seasons, $G_{p,\mathrm{crop}}$ is the total days across all growing seasons for the crop

$$f_{\text{thermal},p,y,\text{crop}} = \begin{cases} \frac{1}{D}\sum_{d=1}^{D} f_{T_{p,d,y,\text{crop}}}, & \text{for } f_{T_{p,d,y,\text{crop}}} = f_{T_{1,p,d,y,\text{crop}}}, f_{T_{2,p,d,y,\text{crop}}} \\ \frac{1}{G_{p,\text{crop}}}\sum_{d=1}^{G_{p,\text{crop}}} f_{T_{p,d,y,\text{crop}}}, & \text{for } f_{T_{p,d,y,\text{crop}}} = f_{T_{3,p,d,y,\text{crop}}}, f_{T_{4,p,d,y,\text{crop}}} \end{cases} \quad (5)$$

where thermal refers to either hot (maximum temperature-based events) or cold (minimum temperature-based events). This means that the exposure rate to extreme temperature is assessed over the full calendar year in phases T1 and T2, but is restricted to the growing season in phases T3 and T4. Defining the exposure rate ($f_{\text{thermal},p,y,\text{crop}}$) in this way allows us to uniformly compare crops and seasons across space, time, and criteria for both hot and cold thermal events.

Phase T5: apply the framework to all years, seasons and crops. We repeat phases T1–T4 for all crops and growing seasons shown in table 2 for the period 1961–2014.

2.3. Hydrologic event exposure

The standardized precipitation-evapotranspiration index (SPEI) [39] is used to define extreme hydrologic events in ARES. Similar to the thermal event construction process outlined in section 2.2, we construct hydrologic events using a multi-phase procedure that is used to winnow from less restrictive to crop-specific extremes. The following are the general steps:

- Step 1: calculate the daily water balance
- Step 2: restrict climate data in time by crop calendars
- Step 3: calculate the monthly SPEI
- Step 4: classify data based on monthly SPEI value
- Step 5: repeat phases H1–H4 for all crops, seasons, and years in the study domain

Note that each step is performed for both the crop-agnostic and crop-specific formulation (e.g. with the crop coefficient). The following are additional details on each of the hydrologic event phases:

Step 1: Calculate the daily water balance. SPEI is based on both precipitation (P) and reference evapotranspiration (ET_0), the difference of which yields the water balance (WB) as defined daily (d) for each pixel (p) via equation (6) [39]

$$\text{WB}_{p,d,y} = P_{p,d,y} - k\text{ET}_{0_{p,d,y}}. \quad (6)$$

where k is the crop coefficient and the reference evapotranspiration is calculated using the Penman-Monteith method [40]. Vicente-Serrano *et al* [39] use k equal to 1 to define a general water balance. Here, we follow the approach of Vicente-Serrano *et al* [39], with the addition of crop-specific k values (see table 2) to determine crop-specific water balances. Thus, we first establish the 'standard' approach to calculate pixel-level SPEI values following Vicente-Serrano *et al* [39], and then additionally develop a 'crop-specific' approach.

Step 2: restrict climate data in time by crop calendars. Similar to phase T3, we restrict the pixels for the water balance analysis to those that have crop calendar information. Note that the 'standard' approach includes all days in the calendar year, which is similar to phases T1 and T2.

Step 3: calculate the monthly SPEI. Daily water balances are aggregated to monthly totals for each pixel. The 'SPEI' package in R is used to calculate SPEI for each pixel and timescale using a log-logistic distribution [41]. Following Zipper *et al* [26], we use 1–3 months for short-term and 12 months for long-term time scales to quantify hydrologic events. A reference period of 1961–1990 is used as this is the same period used for baseline suitability in the Global Agro-Ecological Zones [42, 43] database that underpins the PCAM dataset [29].

Step 4: classify data based on monthly SPEI values. SPEI values can be either positive or negative [39], which enables us to categorize results as either 'wet' (SPEI $>$ 0) or 'dry' (SPEI $<$0). These values can be further classified as 'normal', 'moderate', 'severe', or 'extreme' (see table S1). 'Abnormal' dryness and wetness are defined for periods of negative and positive values outside of the normal range, respectively. We consider hydrologic events to be any month where the SPEI value is categorized as abnormal (i.e. moderate, severe or extreme; $|\text{SPEI}| > 1$) and extreme ($|\text{SPEI}| > 2$).

The binary construct for classifying monthly SPEI values with the standard approach is presented in equation (7) as:

$$f_{1,\text{hydro,type},p,m,y} = \begin{cases} 1, & |\text{SPEI}_{p,m,y}| > |\text{SPEI}_{\text{type}}| \\ 0, & \text{otherwise} \end{cases} \quad (7)$$

where $f_{1,\text{hydro,type},p,m,y}$ is the standard (i.e. non-crop-specific) definition of SPEI, and pixel (p), month (m), and year (y) are tracked. Note that hydro refers to

either wet or dry extremes and type is either the abnormal or extreme category.

The indicator for crop-specific monthly SPEI is shown in equation (8), below:

$$f_{2,\text{hydro,type},p,m,y} = \begin{cases} 1, & |\text{SPEI}_{p,m,y,\text{crop}}| > |\text{SPEI}_{\text{type}}| \;\&\; m_{p,\text{crop,PS}} \leq m \leq m_{p,\text{crop,HE}} \\ 0, & \text{otherwise} \end{cases} \tag{8}$$

where all variables follow those in equation (7). We use the crop calendars from Sacks *et al* [34] to determine active agricultural months. The first month ($m_{p,\text{crop,PS}}$) and last month ($m_{p,\text{crop,HE}}$) form the bounds of the growing season for the crop-specific hydrologic events. The monthly events are aggregated to form the annual hydrologic event exposure rate as shown in equation (9):

$$f_{\text{hydro,type},p,y,\text{crop,method}} = \begin{cases} \frac{1}{M}\sum_{m=1}^{M} f_{1,\text{hydro,type},p,m,y} \\ \\ \frac{1}{A_{p,\text{crop}}}\sum_{m=1}^{A_{p,\text{crop}}} f_{2,\text{hydro,type},p,m,y} \end{cases} \tag{9}$$

where method refers to either the standard or crop-specific approach, M are the number of months in the calendar year ($= 12$), and $A_{p,\text{crop}}$ is the number of months in the agricultural growing season for a given crop in pixel p. For congruency with the thermal phases, we refer to phases H1 and H2 as the standard approach's abnormal and extreme types, respectively, that are based on the full calendar year. Similarly, phases H3 and H4 refer to the crop-specific approach's abnormal and extreme types, respectively, that are restricted to the growing season.

Step 5: apply the framework to all years, growing seasons and crops. We repeat steps 1–4 for all crops and growing seasons shown in table 2 for the period 1961–2014.

2.4. Spatially aggregating pixels

The core output of the ARES model is a global gridded dataset of crop-specific exposure to thermal and hydrologic extremes. We anticipate that it will also be helpful to determine these extremes at the country and global spatial scales. To aggregate the pixels from ARES we use the PCAM dataset [29] to construct summary exposure rates at the global, country, and pixel spatial resolutions. To do so, we use three weighting schemes to combine exposure rates such that results are weighted according to the most likely locations of each crop.

The first scheme occurs within the pixel. We use the likelihood fractions provided by PCAM [29] to obtain relative weights amongst crops in pixel p. This enables us to combine similar weather events in pixel p without double counting to derive comprehensive activity for a given weather event across all crops in the pixel. The second scheme involves aggregating weather events to perform country-level analysis. We also employ the data from PCAM [29] to obtain relative weights amongst a country's pixels for a given crop. In this way, we obtain aggregated values for each country via weighted averaging. Global and regional (e.g. East Asia & Pacific) summaries are weighted averages based on country-level results where the weights are determined by the number of agricultural pixels according to PCAM [29].

2.5. Model assumptions

The ARES modeling framework relies on a few critical assumptions. First, restricting the climate data in time is based on the crop calendars provided by Sacks *et al* [34]. We assume the agricultural year begins on the first day of the planting seasons and continues through the last day of the harvest season. This approach may not be fully representative of the length and actual active days for a given crop. Recent advances in modeling crop calendars in a dynamic fashion for staple crops have taken place at the regional [44] and global scales [45]. However, the calendars provided by Sacks *et al* [34] allow us to consider time constraints for crops beyond maize, rice, soybeans, and wheat, while also providing global coverage. Our approach would be improved with a time-varying database of these crop calendars. An additional assumption concerns multi-cropping and 'alternative' growing seasons. Here, we use the term 'alternative' to describe a crop that has both a main ('spring') and winter seasons (e.g. barley and wheat). We assume that a crop with multiple seasons will have plantings for each season every year.

Additionally, we had to make some assumptions to match the spatial resolution of supporting datasets. The native resolution of Sacks *et al* [34] and PCAM [29] is 0.5°. We downscaled the data to the 0.25° resolution by assuming the values of the finer mesh are equivalent to the coarser mesh. However, it is possible that the constituent PCAM pixels actually have different likelihood estimates, which affects the subsequent weighting scheme that are used to develop country-level and global aggregate exposure rates.

The thermal thresholds are developed from a literature search. Values from multiple growing domains are averaged together. In comparison to the

approach by Teixeira *et al* [27], we consider the full length of the growing season to understand the totality of the crop's exposure to extreme conditions. For the crop coefficients, the values presented in table 2 are averaged across different regions to obtain a global value. This approach assumes that the crop-specific thresholds are uniform in time and space. It is likely that regional crop varietals will have different climate adaptations, leading us to incorrectly estimate extremes for that crop in some places. Similarly, advances in genetic crop breeding has likely changed the crop thresholds over time. We do not capture threshold dynamics.

2.6. Model assessment

We compare ARES with another disaster and extreme weather event database. ARES outputs are compared at the global and national spatial scales to the EM-DAT database [46]. EM-DAT is a well-established global disaster database that has been used in previous agriculturally focused studies involving extreme events [11, 47–50]. We obtain date ranges of occurrences for floods, droughts, heat waves, and cold waves from EM-DAT, as these are the closest event types to ARES. A daily time series for each country-event type pair is developed using a binary construct indicating if the given day for the country experienced an event. These occurrences are summed across the year and divided by the total number of days in the year to derive each country's event exposure rate based on EM-DAT data. A global time series is constructed by calculating a weighted average based on the country-level exposure rates. The weights are based on each country's contribution to global landmass, excluding Antarctica.

Four quantitative metrics are used to compare ARES with EM-DAT at aggregate country and global scales: (1) mean absolute error (MAE); (2) mean square error (MSE); (3) Mann-Kendall's Z-statistic [51, 52]; and (4) Sen-Theil estimate, $\hat{\beta}_{\mathrm{TS}}$ [53, 54]. The first two metrics allows us to directly compare the outputs of the two datasets. The last two metrics enable comparisons of the long-term trends of the two datasets. In particular, the Z-statistic determines the general direction of the trend (e.g. Z-statistic < 0 is a negative trend). $\hat{\beta}_{\mathrm{TS}}$ is an estimate of the trend's magnitude and can be interpreted as an estimate of the long-term change. The p-value from $\hat{\beta}_{\mathrm{TS}}$ was used to determine statistical significance. For clarity, we convert the $\hat{\beta}_{\mathrm{TS}}$, MAE, and MSE results to percentages. Note that the ARES results used in this comparison are global and country-level results that have been aggregated across all crops. We apply all four metrics across our entire time domain at both the country and global levels.

2.7. Model trend analysis

We evaluate national and global changes in crop exposure rates over time. We quantify the precision of ARES outputs by determining the percent difference between criteria using the annual global crop-specific exposure rates. There are three comparisons for thermal events: restriction to the generic optimum versus restriction to the crop-specific optimum; restriction to the crop-specific optimum versus the additional inclusion of restriction to the crop calendar; and restriction to the crop calendar versus restriction to the crop-specific extreme threshold. There are two comparisons for hydrologic events: the standard approach's abnormal rating versus the standard approach's extreme rating; and the crop-specific approaches abnormal versus extreme ratings. Also, the percent change in the number of active pixels is tabulated. We perform these calculations for both the year 2000 as a cross-section as well as the entire time domain.

We set 1961 as the baseline year to determine changes over time, as this is the first year of the study. Impact by crop is estimated by calculating the percent difference in global crop-specific event exposure rates between the given year and the baseline year. We also tabulate Mann-Kendall's Z-statistic [51, 52] and the Sen-Theil estimate $\hat{\beta}_{\mathrm{TS}}$ [53, 54] using the global aggregate crop-specific time series. These sets of statistics enable us to quantify which crop is being affected by which extreme event type the most from a long term perspective (i.e. $\hat{\beta}_{TS}$) and from a year-over-year perspective. We also calculate the relative change on a regional scale. To do so, countries are matched to their region using the `cshapes` package [55]. Regional exposure rate estimates are weighted averages that are developed in the same fashion as the global aggregate estimates.

3. Results

The key results of the ARES framework are presented here. First, we present results on how our understanding of extreme events in agriculture changes as we increasingly refine the definition of an extreme event. In other words, we explore how moving from a generic definition to a crop-specific definition changes our assessment of climate extremes in agriculture. Then, we evaluate trends and drivers of change for crop-specific exposure to extremes. Lastly, ARES results are compared with the EM-DAT database. Throughout this section, 'hot', 'cold', 'wet', and 'dry' are used as a short-hand reference for extreme heat, cold, wetness, and dryness events.

3.1. Moving from generic to crop-specific extremes

Here, we assess how our understanding of extremes changes as we 'peel the onion' and move from crop-agnostic to crop-specific definitions of extremes (e.g. from T1 to T4; see sections 2.2 and 2.3). The spatial extent and the mean exposure rate (i.e. the fraction of the year affected) change with increased refinement of the definition of climate extremes. Figure 2 provides

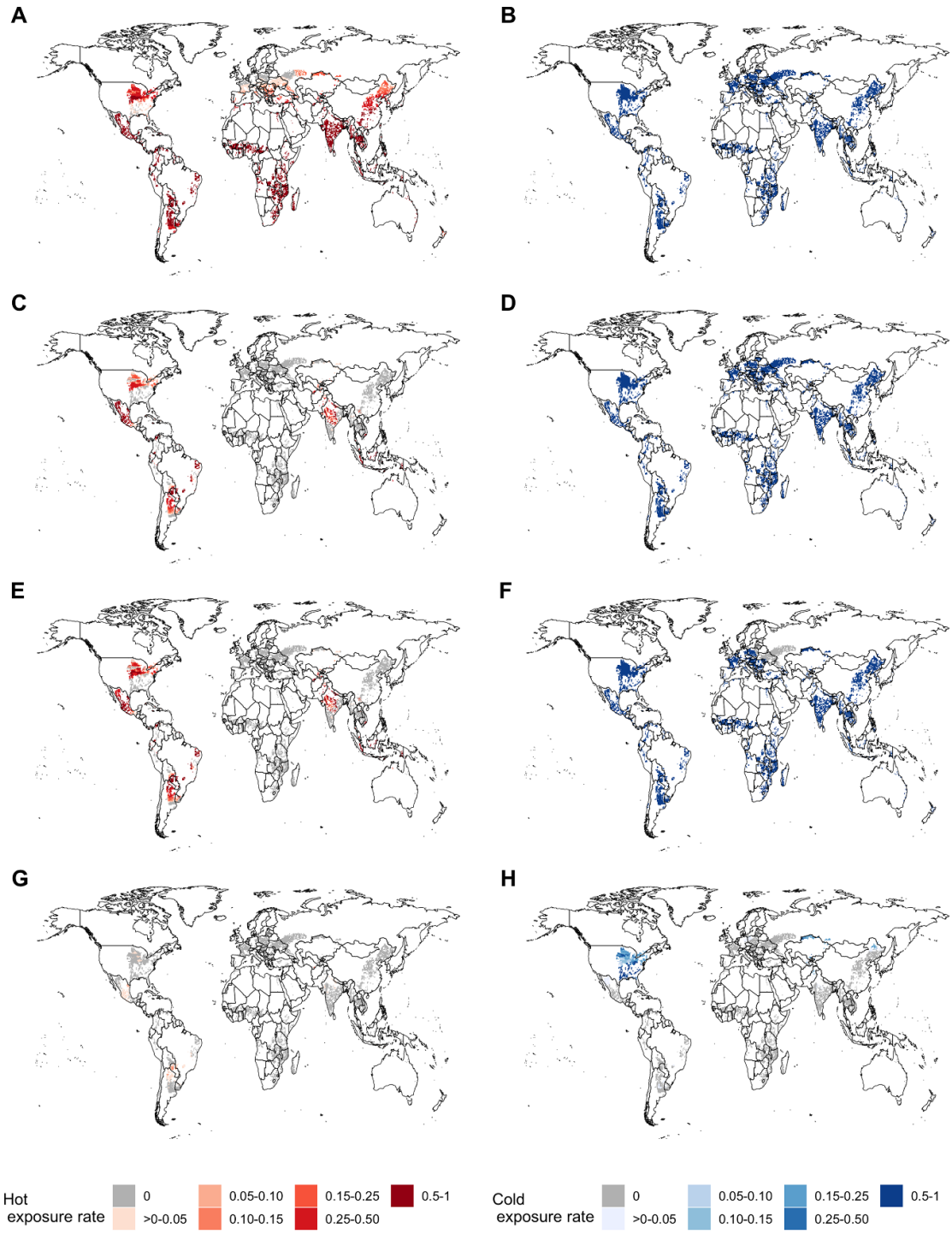

Figure 2. Maps of temperature extremes for maize. The left column shows extreme heat and the right column shows extreme cold for the year 2000. Each row illustrates the winnowing process: row 1 is the most conservative optimum value across all crops; row 2 is the crop-specific optimum temperature; row 3 restricts to the growing season; and row 4 is the crop-specific extreme threshold within the growing season.

an example of how the thermal extremes are winnowed for maize when increasingly refined thresholds are applied in the year 2000. In figure 2(A), 92.6% of maize pixels are exposed exposed with a mean exposure rate of 0.454 (phase T1). The percentage of exposed pixels is reduced to 28.6% in figure 2(C), with a mean exposure rate of 0.086. When we restrict to the maize growing season in figure 2(E), the percentage of exposed pixels is further reduced to 27.9% with a mean exposure rate of 0.103. Finally, restricting to maize's maximum temperature threshold (i.e. 42.0 °C; see table 2), leave 7.2% exposed pixels and a mean exposure rate of 0.002. Comparable values of 'peeling the onion' for cold events for maize in figure 2 are provided in table S6B.

Similarly, figure 3 shows how the various hydrologic criteria vary in space. The progression for dry events is shown in figures 3(A), (C), (E), and (G);

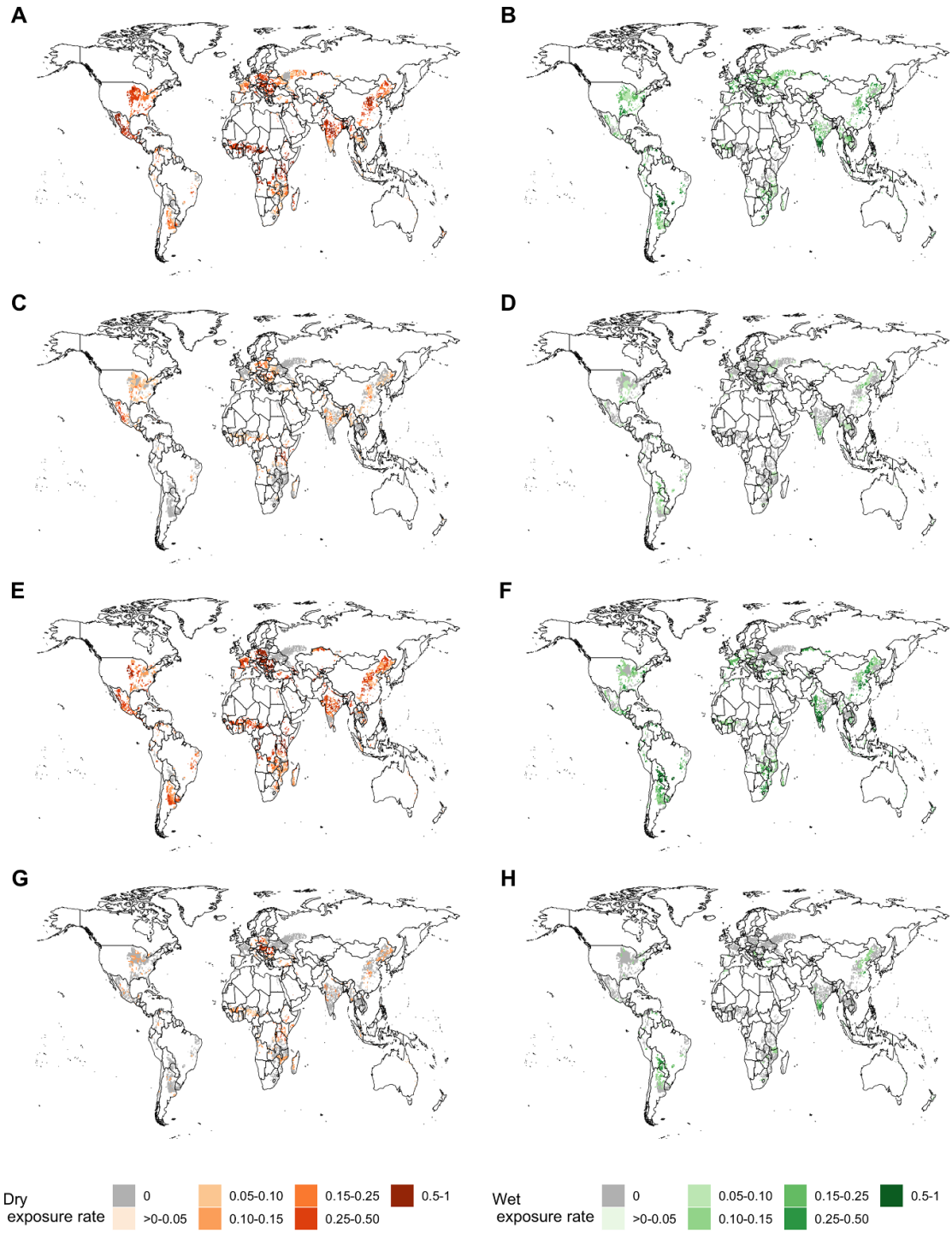

Figure 3. Maps of moisture extremes for maize. The left column shows dry conditions and the right column shows excess moisture for the year 2000. Each row illustrates the winnowing process. The top two rows do not incorporate crop-specific coefficients in the water balance calculations, whereas the bottom two rows do. Rows one and three are based on SPEI > 1, and rows 2 and 4 are based on SPEI > 2.

wet events are shown in figures 3(B), (D), (F), and (H). Note that restricting to the growing season of maize focuses the definition to the most impactful time period for agriculture and the exposure rate to drought increases in certain locations (e.g. note increased red in select areas in figure 3(E) from figure 3(A); the mean intensity changes from 0.258 to 0.229). However, applying the more restrictive crop coefficient in figure 3(G) dampens the quantification of dry event exposure for maize (mean intensity goes from 0.229 in figure 3(E) to 0.049 in figure 3(G). Application of the maize crop coefficient has a similar dampening effect in figure 3(H). More detailed walk-throughs of how the changing criteria affect the spatial extent and exposure rate are provided in the supplementary information (SI). Overall, the

inclusion of crop-specific criteria affects both the magnitude of the exposure rate as well as the fraction of exposed pixels.

Winnowing from generic to crop-specific events changes our assessment by type of weather extreme:

- **Hot:** On average (across all crops) there is a 47.5% reduction in the exposure rate and a 27.9% reduction in affected pixels when we move from the generic to the crop-specific optimum temperature (phase T1 to T2). There is an 11.3% increase in mean exposure rate when we restrict to the crop calendar (phase T2 to T3). There is a relatively sharp reduction (86.9%) in exposure rate when the crop-specific maximum temperature is applied across all crops (phase T3 to T4). Exposure rates for cassava (99.6%), groundnuts (98.6%), and millet (99.7%) show the greatest reductions when a crop-specific threshold is used. Similarly, millet (92.1%), yams (92.7%), and cassava (91.1%) have the largest reduction in the spatial area experiencing heat. Maize, rice, soybeans, and wheat also exhibit over 50% declines in both spatial extent and exposure rate when a more conservative threshold is applied.
- **Cold:** On average there is a 92.1% and 72.6% reduction in exposure rate and percent of pixels affected, respectively, across all crops when using the final crop-specific criteria compared to the generic optimum (phase T1 to T4). Unlike hot events, crops generally did not experience an increase in exposure rate when transitioning from the generic optimum temperature threshold to the crop-specific optimum when using the minimum temperature threshold (phase T1 to T2). For maize, rice, soybeans, and wheat, exposure rates were reduced by 82.3%–98.8%, and the percentage of pixels affected were reduced by 48.3%–93.7% as the criteria became more stringent (phase T1 to T4).
- **Wet:** There is a 5.9% reduction in exposure rate and a 23.6% decline in the fraction of exposed pixels on average (across all crops), when comparing the standard and crop-specific extremes (phase H2 to H4). Approximately 52.9% (= 9/17) of crops saw an increase in exposure rate when the crop-specific extreme definition is used versus the standard approach (phase H2 to H4). This means that, in these cases, the standard approach underestimates the wet exposure rate. Conversely, 82.3% (= 14/17) of crops had a reduction in the fraction of exposed pixels based on the crop-specific approach compared to the standard approach (phase H2 to H4). Thus, for extreme wet events, the standard approach could underestimate exposure rate, yet overestimate the spatial extent of exposure.
- **Dry:** There is a 17% reduction in exposure rate and a 28.3% decline in the fraction of exposed pixels (across all crops), when comparing the standard and crop-specific approaches (phase H2 to H4). Unlike the wet hydrologic events, all crops exhibit declines in percentage of pixels affected when using the crop-specific approach (phase H2 to H4). With the exception of rice, the remaining crops also show reductions in exposure rates (phase H2 to H4). This means that the standard SPEI approach (i.e. that does not account for crop coefficients) for defining dry events may overestimate both the exposure rate and spatial extent for almost all crops in this study.

This highlights that there can be substantial differences in the magnitude and potential spatial extent of extreme weather events when crop-specific physiology is taken into account. Some crops are affected more than others as the definition of climate extremes changes. Millet (−99.97%), rapeseed (−63.5%), rye (−58.9%), and yams (−99.99%) experience the largest reduction in exposure rate for hot, dry, wet, and cold extremes, respectively. Millet (−99.9%) and rye (−77.7%) have the largest reduction in exposed pixels for cold and dry events, respectively. Yams have significant reductions in exposed pixels for both hot (−99.1%) and wet (−77.1%) events.

3.2. Crop-specific exposure over time

Figure 4 shows the relative change over the study period for hot, cold, wet, and dry events for the major staple crops (i.e. maize, rice, soy, and wheat). Wheat exhibits the largest increase in exposure to extreme wetness, while soy shows increased exposure to heat, particularly since the year 2000. All staple crops exhibit the largest increase in dry conditions over the study domain (see figure 4 for 'dry'). Figure 5 shows how barley, cassava, groundnuts, and millet change over time. Cassava has the most exposure to cold, which fluctuates over time. Barley shows a steady increase in exposure to both hydrologic extremes (e.g. both 'dry' and 'wet' in figure 5). Relative change plots are provided for all other crops in this study in the SI (see figures S16 and S17).

For extreme hot events, 41.2% of crops have an increase in their relative change in exposure rate. Fewer crops exhibit increased exposure to heat with the relative change metric than with $\hat{\beta}_{TS}$ (76.7%). Table 3 shows that cassava (172%) has the highest relative increase in extreme heat, whereas potatoes (0.16%) has the highest long-term rate of change. Over half (52.9%) of the crops have a decrease in their exposure to extreme cold over the study domain. Sunflowers (292%) and rapeseed (0.23%) witness the largest increase in extreme cold through relative change and $\hat{\beta}_{TS}$, respectively. All crops show increased exposure to extreme dry events. This is shown by the positive values for Z and $\hat{\beta}_{TS}$: $\hat{\beta}_{TS}$ is statistically significant for dryness in all crops. Soybeans (883%) have the largest increase in exposure to extreme dryness

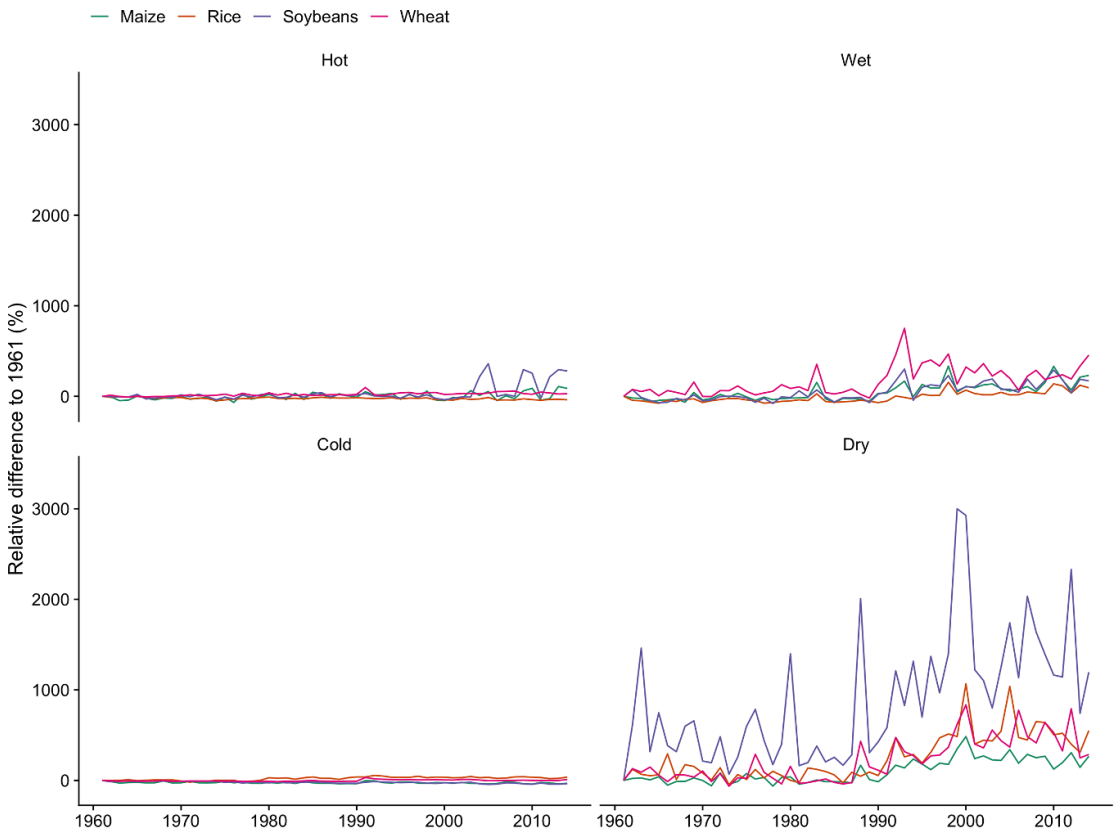

Figure 4. Relative change (%) in the global crop-specific exposure rate. Note the baseline year is 1961. Extreme temperature and moisture events are shown for maize, rice, soybeans, and wheat.

Figure 5. Relative change (%) in the global crop-specific exposure rate. Note the baseline year is 1961. Extreme temperature and moisture events are shown for barley, cassava, groundnuts, and millet.

Table 3. Relative change by crop for the period 1961–2014 for A) thermal and B) hydrologic events. The relative change is calculated using 1961 as the baseline year and values presented are averaged across the entire study domain.

A. Thermal

	Hot				Cold			
	μ	Z	$\hat{\beta}_{TS}(\%)$	Relative change (%)	μ	Z	$\hat{\beta}_{TS}(\%)$	Relative change (%)
Barley	0.037	4.86	0.023^{***}	14.9	0.086	2.81	0.025^{**}	2.0
Cassava	0.001	3.24	0.001^{**}	172.2	0.000	−3.82	0^{***}	−23.4
Groundnuts	0.008	1.16	0.003	−17.6	0.026	−4.09	-0.006^{***}	−11.0
Maize	0.003	2.34	0.003^{*}	−0.1	0.039	−2.91	-0.011^{**}	−24.7
Millet	0.000	1.69	0	−30.8	0.001	2.92	0.002^{**}	89.9
Oats	0.163	5.45	0.082^{***}	−0.8	0.131	3.67	0.089^{***}	16.1
Potatoes	0.224	6.34	0.164^{***}	17.5	0.038	4.49	0.027^{***}	23.1
Rapeseed	0.065	0.69	0.008	−17.8	0.182	4.28	0.229^{***}	45.3
Rice	0.071	−4.46	-0.043^{***}	−24.3	0.010	5.07	0.007^{***}	20.2
Rye	0.031	−0.78	−0.003	−13.4	0.101	−6.86	-0.082^{***}	−19.8
Sorghum	0.023	−2.15	-0.006^{*}	−9.8	0.055	−3.21	-0.011^{**}	−11.8
Soybeans	0.023	2.34	0.011^{*}	34.6	0.059	−6.79	-0.042^{***}	−22.2
Sugarbeets	0.036	4.83	0.032^{***}	15.4	0.051	4.68	0.052^{***}	22.6
Sunflower	0.001	3.64	0.002^{***}	168.9	0.051	6.43	0.091^{***}	292.3
Sweet potatoes	0.016	−0.73	−0.003	−5.0	0.025	−5.52	-0.013^{***}	−18.7
Wheat	0.092	6.34	0.06^{***}	21.8	0.131	3.07	0.029^{**}	−1.1
Yams	0.028	0.49	0.003	−29.2	0.000	−2.95	0^{**}	−50.4

B. Hydrologic

	Dry				Wet			
	μ	Z	$\hat{\beta}_{TS}(\%)$	Relative change (%)	μ	Z	$\hat{\beta}_{TS}(\%)$	Relative change (%)
Barley	0.014	5.62	0.046^{***}	299.3	0.015	5.18	0.038^{***}	141.1
Cassava	0.021	6.48	0.07^{***}	84.4	0.022	4.89	0.058^{***}	−24.9
Groundnuts	0.016	5.58	0.046^{***}	157.1	0.022	4.88	0.059^{***}	−0.8
Maize	0.017	5.48	0.048^{***}	104.3	0.020	5.54	0.052^{***}	46.7
Millet	0.011	5.09	0.029^{***}	113.7	0.015	3.88	0.029^{***}	−18.6
Oats	0.014	4.86	0.046^{***}	128.7	0.017	5.73	0.043^{***}	285.0
Potatoes	0.015	5.73	0.043^{***}	311.5	0.014	4.85	0.026^{***}	221.5
Rapeseed	0.013	5.03	0.042^{***}	117.4	0.016	4.51	0.033^{***}	44.4
Rice	0.019	5.66	0.058^{***}	255.4	0.024	5.52	0.06^{***}	−8.5
Rye	0.011	4.46	0.032^{***}	223.6	0.012	6.13	0.039^{***}	99.5
Sorghum	0.016	5.34	0.041^{***}	169.8	0.021	5.16	0.056^{***}	86.5
Soybeans	0.015	4.34	0.036^{***}	883.3	0.019	5.18	0.052^{***}	49.3
Sugarbeets	0.015	4.57	0.05^{***}	246.2	0.016	5.55	0.041^{***}	277.8
Sunflower	0.014	5.15	0.042^{***}	708.8	0.018	6.15	0.057^{***}	38.6
Sweet potatoes	0.020	5.89	0.065^{***}	198.3	0.018	4.85	0.041^{***}	16.5
Wheat	0.014	5.03	0.043^{***}	224.7	0.015	4.73	0.028^{***}	168.9
Yams	0.025	5.64	0.07^{***}	671.7	0.017	3.01	0.028^{**}	−43.2

$^{***}p < 0.001$, $^{**}p < 0.01$, $^{*}p < 0.05$

(see table 3). Many crops also are increasingly exposed to wet events: 71% of crops have increased via the relative change metric, compared with all crops showing an increase in $\hat{\beta}_{TS}$. Oats (285%) and rice (0.06%) have the greatest increase in extreme wet events based on the relative change and long-term change, respectively.

Regional values are provided to hone in on the specific areas that have witnessed the largest changes in exposure by crop. Figure 6 shows rice's exposure to each weather extreme by world region (additional crops are provided in the SI in figures S18–S33). The relative change in exposure rates by region are much higher than global values, due to the very small values in the baseline year (tables S9 and S10). Europe & Central Asia have the largest increases in thermal extremes. These increases are in contrast to the substantially smaller relative changes experienced by sub-Saharan Africa for both hot and cold events as well as the Middle East & North Africa for cold events and North America for hot events. For cold events, sunflowers, maize, and oats are most exposed in this region. For hot events, potatoes in Europe & Central Asia, wheat in the Middle East & North Africa, rapeseed in East Asia & Pacific, sunflowers in North America, and millet in South Asia

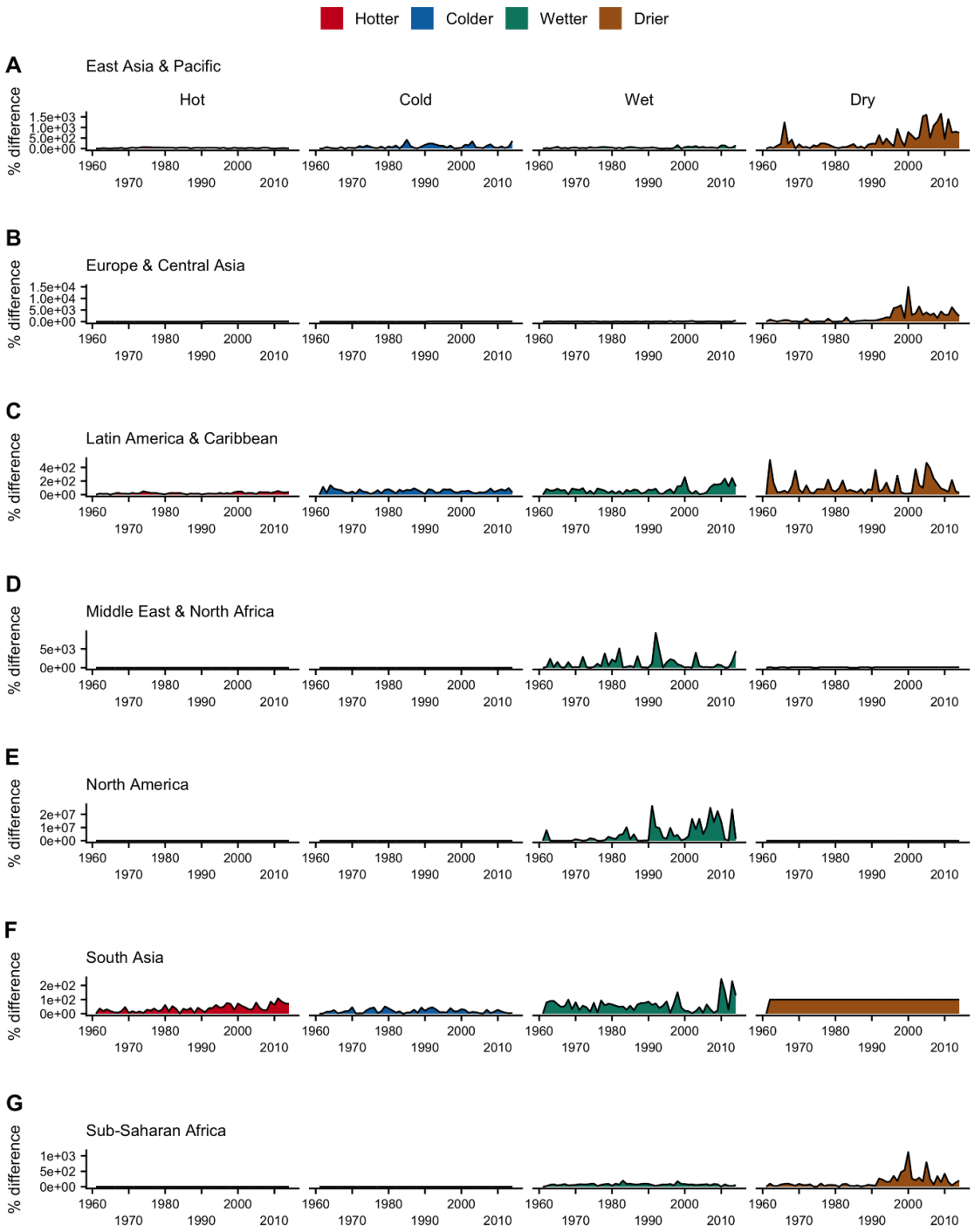

Figure 6. Regional time series of the relative change (%) in exposure rate by extreme weather event for rice. Note the baseline year is 1961.

are increasingly exposed. Sugarbeets and potatoes in the Middle East & North Africa and Latin America & Caribbean regions are most impacted by extreme wet events. However, rice in North America is estimated to be the region and crop most impacted by extreme wet events. Groundnuts, barley, and potatoes in the South Asia region, in addition to soybeans in North America, have the highest relative change in extreme dryness.

3.3. Comparison between ARES and EM-DAT

We map extremes by weather type calculated with ARES and EM-DAT for comparison in figure 7. Note that ARES is designed to specifically quantify extremes in agriculture, with a particular emphasis on crop-specific extremes. Conversely, EM-DAT is a well-established database of extreme weather events, but it is not specifically developed to capture agricultural extremes. As such, the two databases capture

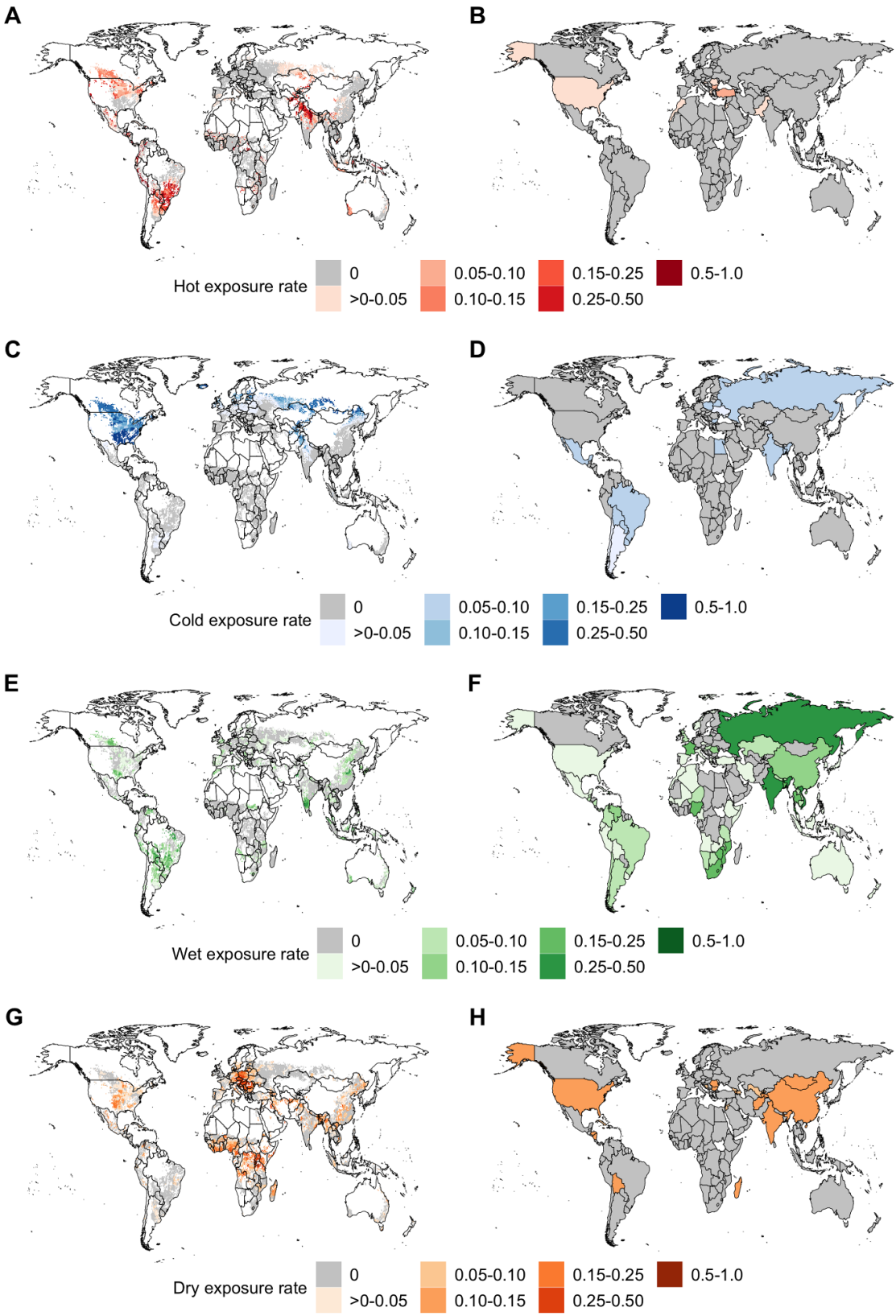

Figure 7. Comparison between gridded ARES (left column) and country-level EM-DAT (right column) exposure rates by weather event for the year 2000. Row one is extreme heat, row two is extreme cold, row three and is extreme wetness, and row four is extreme dryness. Note that ARES reports crop-specific extremes while EM-DAT is not restricted to agricultural hazards.

different events and a comparison between the two is not a true 'apples to apples' comparison. Additionally, EM-DAT relies on countries to report extreme events in order to incorporate them into the database, which means that biases in reporting will exist in the data, including under-representation of countries that do not have the capacity to measure and report such events. However, EM-DAT is the most comprehensive

database of weather extremes and is widely used by the environmental research community.

The approach that we have developed here in the ARES model provides increased precision for agricultural extremes. Notably, weather extremes in ARES are specifically defined by the physiological thresholds of crops. Conversely, events in EM-DAT are likely those that have the largest financial impact, which may or may not occur in agriculture. ARES applies a consistent definition of extremes throughout the entire study domain to climate data that is not biased by weather impact. Reporting procedures have likely changed in time, making it difficult to compares extremes over time in EM-DAT. Figure 7 also shows that ARES produces gridded maps of extremes (see figures 7(A), (C), (E), and (G)), while EM-DAT extremes are lumped to the country spatial scale (see figures 7(B), (D), (F), and (H)). This enables us to pick up on sub-national events, such as extreme heat in Northern India and drought in Eastern Europe and Africa, which is not captured by the EM-DAT data (see figures 7(B), (H)). We provide cross-sectional comparison between ARES and EM-DAT in figure 7, but note that we compare both databases for the entire study domain the SI. Additional details on how ARES and EM-DAT compare with one another are provided in the SI (see section 3 and tables S11–S13).

4. Discussion

4.1. Comparison with prior studies

This paper builds upon the literature that seeks to understand the weather conditions crops have historically experienced globally. Here, we compare ARES output to prior work by Gourdji *et al* [10] and Zhu and Troy [12], who also use crop-specific thresholds to define their thermal events. However, this study distinguishes itself by conducting the analysis at a finer spatial resolution (i.e. 0.25° versus 0.5° [10] and 1° [19]), for more crops (i.e. 17 versus 4), and incorporating annually varying crop-specific land use information versus fixed crop locations. We also look at both tails of temperature and moisture extremes (e.g. too hot/cold and too wet/dry).

Gourdji *et al* [10] assessed the exposure of maize, rice, soybean and wheat to critically high temperatures during the growing season from 1980 to 2011. Importantly, Gourdji *et al* [10] show a weak correspondence between mean growing season temperature and exposure to extreme heat, emphasizing the importance of quantifying weather extremes separately, as we do in this study. Gourdji *et al* [10] find increasing exposure to extreme heat over the past few decades for wheat in Central and South Asia as well as South America, which compares well with our findings (see figure 7(A) and supporting information). Gourdji *et al* [10] additionally project the exposure of the staple crops to high temperature in the future (i.e. through the 2050 s), which we do not do here. However, we do build on the work by Gourdji *et al* [10] by including both temperature extremes (e.g. extreme cold in addition to extreme heat) and moisture extremes (e.g. too wet and too dry) across a longer historical period.

Zhu and Troy [12] assessed agriculturally relevant climate extremes during the growing season for maize, wheat, soybean, and rice from 1951 to 2006. One metric used by Zhu and Troy [12] is growing degree days (GDD), which is the integral of temperature above a threshold temperature for the staple crops; see table 1 of Zhu and Troy [12]. We extend this approach by normalizing the number of days exceeding the crop-specific threshold by the number of days in the calendar or growing year (see phase T4 in section 2.2). The added step enables comparison across different crops and regions by accounting for both crop and spatial variations in growing seasons. An additional critical difference between this work and Zhu and Troy [12] is our modification of SPEI to incorporate crop-specific water demands with crop coefficients (e.g. k; see section 2.3) instead of the Palmer Drought Severity Index (among other metrics) to estimate moisture extremes.

Our results compare favorably with Zhu and Troy [12]. Both studies find that there have been more dry events, particularly since the 1980s, and there is generally good geographic agreement, such as more drought in East Asia. Additionally, both studies show that there has been an increase in exposure to hot temperatures for wheat and soy. Our results diverge for extreme heat in maize and rice. This is likely due to the different temperature thresholds used. Zhu and Troy [12] use a threshold of 30°C for maize and rice, while ARES uses 42.0°C for maize and 35.4°C for rice. We associate the lack of warming trend in this study to the higher maximum temperature thresholds for these crops compared to Zhu and Troy [12].

4.2. Limitations in the ARES database and approach

There are several limitations in the methodology of ARES that limit how it should be used. Farmer adaptations to climate change and weather extremes are difficult to quantify and are not captured by our approach. Importantly, we do not consider how crop physiological thresholds change with time. Genetic breeding of crops means that specific crops may develop different tolerance levels that we do not capture in this study. Additionally, we do not account for spatial variations in crop thresholds. Different growing regions may grow different varietals of the same crop – with different abilities to withstand weather extremes – that our approach does not consider. The same is true for sowing and planting dates. Temporal and spatial changes in crop growing seasons are not captured in this study and represent an important future research area.

Due to data limitations, we do not estimate exposure to extremes for irrigated vs. rainfed crop agriculture. Crops that have access to irrigation will likely not have their yields impacted following exposure to climate extremes as much as rainfed crops. This is because irrigation has been shown to buffer the impact of climate extremes on crop yields [17, 19, 24]. Unfortunately, global databases on irrigation water use by crop are not available, which is what would be needed for our crop-specific study. We do not capture irrigation expansion over time, another important adaptation to climate change and weather extremes. This is a shortcoming of our approach and model output that should caution its use.

The current framework does not consider compound exposure (e.g. extreme heat and dryness occurring simultaneously). Future work could extend the ARES framework to evaluate crop-specific compound events. The crop-specific locations used within ARES are themselves estimates, and future efforts to collect agricultural locations through government censuses through time would enhance reliability. These improvements would enable researchers to better determine the drivers of changes in agricultural extremes.

4.3. Future research directions

Future research could improve on the limitations that we outlined in section 4.2. For example, information on time-varying crop physiological thresholds could be used to develop more precise estimates of crop exposure to extremes. The specific varietals used in different growing regions could be used to spatially vary the thresholds used by ARES. Understanding how farmers adapt to weather extremes by adopting new crop varietals is an important area of future research. Relatedly, farmers can adapt to extreme weather by choosing to grown certain crops in different locations. This is another important area of ongoing research [56] that future applications of ARES could potentially contribute to. Future work could also examine projected climate extremes by crop.

This study quantifies the exposure of specific crops to extreme weather during the growing season, because these events may negatively impact yields. By definition, our climate thresholds should capture negative yield anomalies, since they were collected from the experimental plant biology literature for this purpose. However, as mentioned in section 4.2 we do not include irrigation in this study due to data limitations–which may limit the influence of weather extremes on crop yield–so future work is needed to link the ARES database with yield impact. Rigorously linking the ARES database with yield data is beyond the scope of the current study, but represents an opportunity for future research. To this end, information on irrigation water use by crop is an important research need for the future.

5. Conclusions

The ARES model framework and database was introduced to comprehensively and consistently evaluate crop-specific exposure to extreme weather for the last half-century. Importantly, we conduct a thorough literature review of agronomic research to incorporate crop-specific weather thresholds into our definition of extreme events (for both temperature and moisture). We integrate these crop-specific attributes with climate data and crop locations to evaluate weather extremes in time and space. The framework used to develop ARES enables systematic comparisons of changes in exposure rates across time, space, and crop with and without crop-specific parameters. ARES allows us to track which countries, crops, and years have had the greatest exposure to extreme weather over time. Importantly, we quantify *exposure* and not necessarily *impact* which makes direct comparison with existing datasets difficult (e.g. with EM-DAT) and highlights the importance of linking exposure with impact (e.g. crop yield and production losses, economic impacts) in future work.

This research represents an advancement in terms of integrating crop characteristics with weather data to establish models of extremes in agriculture. Critically, we make the ARES model output available with this publication, to enable future research to build on these efforts. Many critical assumptions and limitations accompany this work (detailed in section 4), so the ARES model output should be used with care.

Data availability statement

All data sources are detailed in table 1 and are publicly available. We gratefully acknowledge these sources, without which this work would not be possible. Output from the Agriculturally-Relevant Exposure to Shocks (ARES) model is available at the persistent link https://doi.org/10.13012/B2IDB-5457902_V1. The DOI for the dataset associated with this study is 10.13012/B2IDB-5457902_V1

Acknowledgments

This material is based upon work supported by the National Science Foundation Grant No. EAR-1534544 ('Hazards SEES: Understanding Cross-Scale Interactions of Trade and Food Policy to Improve Resilience to Drought Risk'), ACI-1639529 ('INFEWS/T1: Mesoscale Data Fusion to Map and Model the U.S. Food, Energy, and Water (FEW) System'), CBET-1844773 ('CAREER: A National Strategy for a Resilient Food Supply Chain'), and DEB-1924309 ('CNH2-L: Feedbacks between Urban Food Security and Rural Agricultural Systems'). Any opinions, findings, and conclusions or recommendations expressed in this material are those of the

author(s) and do not necessarily reflect the views of the National Science Foundation. The Gies College of Business contributed support to MK through the Office of Risk Management & Insurance Research (ORMIR) Faculty Fellowship. NDJ is thankful for the support from the Diversifying Faculty in Illinois fellowship. This paper benefitted from the valuable feedback of Ximing Cai, Kathy Baylis, and three anonymous reviewers.

ORCID iDs

Nicole D Jackson https://orcid.org/0000-0002-3814-9906
Megan Konar https://orcid.org/0000-0003-0540-8438
Justin Sheffield https://orcid.org/0000-0003-2400-0630

References

[1] Chambers R G and Pieralli S 2020 The sources of measured US agricultural productivity growth: weather, technological change and adaptation *Am. J. Agric. Econom.* **102** 1198–226
[2] Chen S and Gong B 2021 Response and adaptation of agriculture to climate change: evidence from China *J. Dev. Econom.* **148** 102557
[3] Liang X Z, Wu Y, Chambers R G, Schmoldt D L, Gao W, Liu C, Liu Y-A, Sun C and Kennedy J A 2017 Determining climate effects on US total agricultural productivity *Proc. Natl Acad. Sci.* **114** E2285–92
[4] Njuki E, Bravo-Ureta B E and O'Donnell C J 2018 A new look at the decomposition of agricultural productivity growth incorporating weather effects *PLoS One* **13** e0192432
[5] Ortiz-Bobea A, Knippenberg E and Chambers R G 2018 Growing climatic sensitivity of US agriculture linked to technological change and regional specializations *Sci. Adv.* **4** eaat4343
[6] Ortiz-Bobea A, Ault T R, Carrillo C M, Chambers R G and Lobell D B 2020 The historical impact of anthropogenic climate change on global agricultural productivity *Nat. Clim. Change* **11** 306–312
[7] Zhong Z, Hu Y and Jiang L 2019 Impact of climate change on agricultural total factor productivity based on spatial panel data model: evidence from China *Sustainability* **11** 1516
[8] Zscheischler J *et al* 2018 Future climate risk from compound events *Nat. Clim. Change* **8** 469–77
[9] Luce C H, Vose J M, Pederson N, Campbell J, Millar C, Kormos P and Woods R 2016 Contributing factors for drought in United States forest ecosystems under projected future climates and their uncertainty *Forest Ecol. Manage.* **380** 299–308
[10] Gourdji S M, Sibley A M and Lobell D B 2013 Global crop exposure to critical high temperatures in the reproductive period: historical trends and future projections *Environ. Res. Lett.* **8** 024041
[11] Lesk C, Rowhani P and Ramankutty N 2016 Influence of extreme weather disasters on global crop production *Nature* **529** 84–7
[12] Zhu X and Troy T J 2018 Agriculturally relevant climate extremes and their trends in the world's major growing regions *Earth's Future* **6** 656–72
[13] Cottrell R S *et al* 2019 Food production shocks across land and sea *Nat. Sustain.* **2** 130–37
[14] Lobell D B, Roberts M J, Schlenker W, Braun N, Little B B, Rejesus R M and Hammer G L 2014 Greater sensitivity to drought accompanies maize yield increase in the US midwest *Science* **344** 516–19
[15] Madadgar S, AghaKouchak A, Farahmand A and Davis S J 2017 Probabilistic estimates of drought impacts on agricultural production *Geophys. Res. Lett.* **44** 7799–807
[16] Zhao C *et al* 2017 Temperature increase reduces global yields of major crops in four independent estimates *Proc. Natl Acad. Sci. USA* **114** 9326–31
[17] Vogel E, Donat M G, Alexander L V, Meinshausen M, Ray D K, Karoly D, Meinshausen N and Frieler K 2019 The effects of climate extremes on global agricultural yields *Environ. Res. Lett.* **14** 054010
[18] Schlenker W and Roberts M J 2007 Nonlinear temperature effects indicate severe damages to US crop yields under climate change *Proc. Natl Acad. Sci. USA* **106** 15594–8
[19] Troy T J, Kipgen C and Pal I 2013 The impact of climate extremes and irrigation on US crop yields *Environ. Res. Lett.* **10** 054013
[20] Zampieri M, Ceglar A, Dentener F and Toreti A 2017 Wheat yield loss attributable to heat waves, drought and water excess at the global, national and subnational scales *Environ. Res. Lett.* **12** 064008
[21] Lobell D B, Hammer G L, McLean G, Messina C, Roberts M J and Schlenker W 2013 The critical role of extreme heat for maize production in the United States *Nat. Clim. Change* **3** 497–501
[22] Ray D K, Gerber J S, MacDonald G K and West P C 2015 Climate variation explains a third of global crop yield variability *Nat. Commun.* **6** 5989
[23] Li Y, Guan K, Schnitkey G D, DeLucia E and Peng B 2019 Excessive rainfall leads to maize yield loss of a comparable magnitude to extreme drought in the United States *Glob. Change Biol.* **25** 2325–37
[24] Ortiz-Bobea A, Wang H, Carrillo C M and Ault T R 2019 Unpacking the climatic drivers of US agricultural yields *Environ. Res. Lett.* **14** 064003
[25] Geng G *et al* 2016 Agricultural drought hazard analysis during 1980–2008: a global perspective *Int. J. Climatol.* **36** 389–99
[26] Zipper S C, Qiu J and Kucharik C J 2016 Drought effects on US maize and soybean production: spatiotemporal patterns and historical changes *Environ. Res. Lett.* **11** 094021
[27] Teixeira E I, Fischer G, van Velthuizen H, Walter C and Ewert F 2013 Global hot-spots of heat stress on agricultural crops due to climate change *Agric. For. Meteorol* **170** 206–15
[28] Monfreda C, Ramankutty N and Foley J A 2008 Farming the planet: 2. Geographic distribution of crop areas, yields, physiological types and net primary production in the year 2000 *Glob. Biogeochem. Cycles* **22** GB1022
[29] Jackson N, Konar M, Debaere P and Estes L 2019 Probabilistic global maps of crop-specific areas from 1961 to 2014 *Environ. Res. Lett.* **14** 094023
[30] Porter J R and Gawith M 1999 Temperatures and the growth and development of wheat: a review *Eur. J. Agron.* **10** 23–36
[31] Hatfield J L and Prueger J H 2015 Temperature extremes: effect on plant growth and development *Weather Clim. Extremes* **10** 4–10
[32] Sheffield J, Goteti G and Wood E F 2006 Development of a 50-yr high-resolution global dataset of meteorological forcings for land surface modeling *J. Clim.* **19** 3088–111
[33] Chaney N W, Sheffield J, Villarini G and Wood E F 2014 Development of a high-resolution gridded daily meteorological dataset over sub-Saharan Africa: spatial analysis of trends in climate extremes *J. Clim.* **27** 5815–35
[34] Sacks W J, Deryng D, Foley J A and Ramankutty N 2010 Crop planting dates: an analysis of global patterns *Glob. Ecol. Biogeogr.* **19** 607–20
[35] Doorenbos J and Pruitt W O 1977 Crop water requirements—FAO irrigation and drainage paper no. 24

Technical Report (Rome: Food and Agriculture Organization of the United Nations)
[36] Doorenboos J and Pruitt W O 1977 Guidelines for predicting crop water requirements *Technical Report* (Rome: Food and Agriculture Organization of the United Nations)
[37] Lobell D B, Bänziger M, Magorokosho C and Vivek B 2011 Nonlinear heat effects on African maize as evidenced by historical yield trials *Nat. Clim. Change* **1** 42–5
[38] Barlow K M, Christy B P, O'Leary G J, Riffkin P A and Nuttall J G 2015 Simulating the impact of extreme heat and frost events on wheat crop production: a review *Field Crops Res.* **171** 109–19
[39] Vicente-Serrano S M, Begueria S and Lopez-Moreno J I 2010 A multiscalar drought index sensitive to global warming: the standardized precipitation evapotranspiration index *J. Clim.* **23** 1696–718
[40] Allen R G *et al* 1998 Crop evapotranspiration-guidelines for computing crop water requirements-fao irrigation and drainage paper 56 *Technical Report* 9
[41] Begueria S and Vicente-Serrano S M 2017 R package: SPEI (available at: http://spei.csic.es/)
[42] Food 2016 Agriculture Organization of the United Nations, and the Int. Institute for Applied Systems Analysis Global agro-ecological zones (available at: http://www.fao.org/nr/gaez/en/)
[43] Fischer G, Nachtergaele F O, Prieler S, Teixeira E, Toth G, Harrij van V, Verelst L and Wiberg D 2012 *GAEZ ver 3.0 Global Agro-ecological Zones Model Documentation* (Food and Agriculture Organization of the United Nations and the International Institute for Applied Systems Analysis) (available at: http://www.fao.org/fileadmin/user_upload/gaez/docs/GAEZ_Model_Documentation.pdf)
[44] Mathison C, Deva C, Falloon P and Challinor A J 2018 Estimating sowing and harvest dates based on the Asian summer monsoon *Earth Syst. Dyn.* **9** 563–92
[45] Minoli S, Egli D B, Rolinski S and Müller C 2019 Modelling cropping periods of grain crops at the global scale *Glob. Planet. Change* **174** 35–46
[46] Guha-Sapir D 2009 EM-DAT: the emergency events database—universite catholique de louvain (UCL)—CRED data retrieved from EM-DAT (available at: http://www.emdat.be/)
[47] Brás T A, Jägermeyr J and Seixas J 2019 Exposure of the EU-28 food imports to extreme weather disasters in exporting countries *Food Security* **11** 1373–93
[48] Krishnamurthy P K, Lewis K and Choularton R J 2014 A methodological framework for rapidly assessing the impacts of climate risk on national-level food security through a vulnerability index *Glob. Environ. Change* **25** 121–32
[49] Minamiguchi N 2005 The application of geospatial and disaster information for food insecurity and agricultural drought monitoring and assessment by the FAO GIEWS and Asia FIVIMS *Workshop on Reducing Food Insecurity Associated With Natural Disasters in Asia and the Pacific* vol 27 p 28
[50] Golian S, Mazdiyasni O and AghaKouchak A 2015 Trends in meteorological and agricultural droughts in Iran *Theor. Appl. Climatol.* **119** 679–88
[51] Mann H B 1945 Nonparametric tests against trend *Econometrica: J. Econometric Soc.* 245–59
[52] Kendall M G 1948 Rank correlation methods
[53] Sen P K 1968 Estimates of the regression coefficient based on Kendall's tau *J. Am. Stat. Assoc.* **63** 1379–89
[54] Theil H 1992 A rank-invariant method of linear and polynomial regression analysis *Henri Theil's Contributions to Economics and Econometrics* (Berlin: Springer) pp 345–81
[55] Weidmann N B and Gleditsch K S 2016 *cshapes: The CShapes Dataset and Utilities* R package version 0.6. (available at: https://CRAN.Rproject.org/package=cshapes)
[56] Sloat L L, Davis S J, Gerber J S, Moore F C, Ray D K, West P C and Mueller N D 2020 Climate adaptation by crop migration *Nat. Commun.* **11** 1243